J Physiol 594.21 (2016) pp 6117–6131

The Journal of Physiology

Organization of flexor–extensor interactions in the mammalian spinal cord: insights from computational modelling

Natalia A. Shevtsova and Ilya A. Rybak

Department of Neurobiology and Anatomy, Drexel University College of Medicine, Philadelphia, PA, USA

Key points

- Alternation of flexor and extensor activity in the mammalian spinal cord is mediated by two classes of genetically identified inhibitory interneurons, V1 and V2b.
- The V1 interneurons are essential for high-speed locomotor activity. They secure flexor–extensor alternations in the intact cord but lose this function after hemisection, suggesting that they are activated by inputs from the contralateral side of the cord.
- The V2b interneurons are involved in flexor–extensor alternations in both intact cord and hemicords.
- We used a computational model of the spinal network, simulating the left and right rhythm-generating circuits interacting via several commissural pathways, and extended this model by incorporating V1 and V2b neuron populations involved in flexor–extensor interactions on each cord side.
- The model reproduces multiple experimental data on selective silencing and activation of V1 and/or V2b neurons and proposes the organization of their connectivity providing flexor–extensor alternation in the spinal cord.

Abstract Alternating flexor and extensor activity represents the fundamental property underlying many motor behaviours including locomotion. During locomotion this alternation appears to arise in rhythm-generating circuits and transpires at all levels of the spinal cord including motoneurons. Recent studies *in vitro* and *in vivo* have shown that flexor–extensor alternation during locomotion involves two classes of genetically identified, inhibitory interneurons: V1 and V2b. Particularly, in the isolated mouse spinal cord, abrogation of neurotransmission derived by both V1 and V2b interneurons resulted in flexor–extensor synchronization, whereas selective inactivation of only one of these neuron types did not abolish flexor–extensor alternation. After hemisection, inactivation of only V2b interneurons led to the flexor–extensor synchronization, while inactivation of V1 interneurons did not affect flexor–extensor alternation. Moreover, optogenetic activation of V2b interneurons suppressed extensor-related activity, while similar activation of V1 interneurons suppressed both flexor and extensor oscillations. Here, we address these issues using the previously published computational model of spinal circuitry simulating bilateral interactions between left and right rhythm-generating circuits. In the present study, we incorporate V1 and V2b neuron populations on both sides of the cord to make them critically involved in flexor–extensor interactions. The model reproduces multiple experimental data on the effects of hemisection and selective silencing or activation of V1 and V2b neurons and suggests connectivity profiles of these neurons and their specific roles in left–right (V1) and flexor–extensor (both V2b and V1) interactions in the spinal cord that can be tested experimentally.

(Received 14 March 2016; accepted after revision 7 June 2016; first published online 13 June 2016)
Corresponding author: I. A. Rybak: Department of Neurobiology and Anatomy, Drexel University College of Medicine, 2900 Queen Lane, Philadelphia, PA 19129, USA. Email: rybak@drexel.edu

DOI: 10.1113/JP272437

Introduction

Coordination of flexor and extensor activity represents a fundamental mechanism underlying almost any motor behaviour including control of posture and different movements, such as reaching and locomotion. During locomotion, flexor and extensor muscles controlling each joint contract repeatedly and in alternation so that each does not interfere with the activity of the other. The alternating contraction of antagonistic muscles requires alternating activity of flexor- and extensor-related neuron populations in the spinal cord controlling the corresponding muscles. This alternating flexor and extensor neural activity in the cord results from specially organized inhibitory interactions that regulate and coordinate many functions from processing of sensory information and sensory–motor integration to rhythm and pattern generation (reviewed by Goulding *et al.* 2014). Recent studies have discovered two groups of genetically identified, inhibitory interneurons, known as V1 and V2b, that are critically involved in alternation of flexor and extensor activity in newborn mice (Zhang *et al.* 2014; Britz *et al.* 2015). Specifically, in the isolated mouse spinal cord, simultaneous abrogation of V1 and V2b interneuron-derived neurotransmission led to synchronization of flexor- and extensor-related activities (Zhang *et al.* 2014). Moreover, mice lacking V1 and V2b inhibition could not move their limbs and experienced marked deficits in limb-driven reflex movements (Zhang *et al.* 2014; Britz *et al.* 2015). Britz *et al.* (2015) have also demonstrated that, although both V1 and V2b neuron types are involved in flexor–extensor alternation, their functional roles are different, and their selective inactivation produces different effects on locomotor activity both *in vivo* and *in vitro*.

The V1 and V2b neurons represent heterogeneous populations of ipsilaterally projecting, inhibitory interneurons in the spinal cord. They both include multiple subpopulations performing different functions at different functional and structural levels of the spinal cord, including recurrent inhibition by Renshaw cells (V1 interneurons), reciprocal inhibition by Ia interneurons (V1 and V2b cells), and afferent inhibition by putative Ib interneurons (V2b cells) (Sapir *et al.* 2004; Alvarez *et al.* 2005; Goulding *et al.* 2014; Zhang *et al.* 2014; Catela *et al.* 2015; Lu *et al.* 2015). In addition, V1 interneurons were shown to be necessary for generating fast locomotor activity, since their selective ablation slowed down the locomotor rhythm in the isolated spinal cord (Gosgnach *et al.* 2006) suggesting that they can play a role in the regulation of locomotor speed at the rhythm generation level (Rybak *et al.* 2015).

The main objectives of this study were to (1) analyse multiple experimental data on the effects of selective silencing and activation of V1 and V2b neurons and, based on this analysis, suggest the possible patterns of V1 and V2b connectivity within the rhythm-generating spinal circuitry; (2) incorporate V1 and V2b neuron populations in the previously developed computational model simulating left–right interactions in the spinal cord (Shevtsova *et al.* 2015) using the proposed connectivity patterns, and (3) validate the proposed connectivity of these neurons and their roles in the network by testing the ability of the resultant extended model to reproduce the results of multiple experiments based on selectively manipulating these neuron types.

Methods

In this computational study we used and extended our previous model of mammalian rhythm-generating circuits that was described in detail in the preceding paper (Shevtsova *et al.* 2015, Model 1). For simplicity, some populations were renamed, which is clear from the model schematic representation and the descriptions provided in the Appendix. The preceding model was extended by incorporating V1 and V2b neuron populations. Similar to the preceding model, the rhythm-generating (RG) populations or centres (RG-F and RG-E) contained 200 neurons each. All other populations, including the incorporated V1 and V2b populations, consisted of 100 neurons each. The detailed description of the single neuron model and synaptic interactions can be found in the preceding paper (Shevtsova *et al.* 2015) and in the Appendix. Neurons in the RG-E and RG-F populations included the following ionic currents: fast sodium (I_{Na}), persistent (slowly inactivating) sodium (I_{NaP}), delayed-rectifier potassium (I_K), leakage (I_L), and excitatory (I_{SynE}) and inhibitory (I_{SynI}) synaptic currents. Neurons in all other populations had I_{Na}, I_K, and I_L and synaptic currents. The V1 and V2a neurons also had an additional channelrhodopsin (ChR) leak-like current I_{ChR} with conductance g_{ChR} and reversal potential $E_{ChR} = 0$ mV (Lin, 2009). This current was zero in control and was used for simulation of optogenetic stimulation of these neurons. The description of all currents, and the corresponding conductances and kinetic parameters are specified in the Appendix, including Tables 1 and 2. To simulate genetic inactivation of V1 and/or V2b neurons, their outputs in the corresponding simulations were set to zero.

Heterogeneity of neurons within each population was provided by random distributions of the leakage reversal potentials E_L (see mean values ± SD for each population in Table 2) and initial conditions for the values of membrane potential and channel kinetics variables. The mean values of the leak reversal potential E_L in RG populations were chosen to provide intrinsic bursting activity in neurons in the flexor RG populations and to let neurons in the extensor RG centres, if isolated, operate in the mode of

Table 1. Steady state activation and inactivation variables and time constants for voltage-dependent ionic channels

Ionic channel	$m_\infty(V)$ and $h_\infty(V)$ (V in mV)	$\tau_m(V)$ and $\tau_h(V)$ (ms)
Fast sodium, Na	$m_{\infty Na} = (1 + \exp(-(V + 34)/7.8))^{-1}$ $h_{\infty Na} = (1 + \exp((V + 55)/7))^{-1}$	$\tau_{mNa} = 0$ $\tau_{hNa} = 20/(\exp((V + 50)/15) + \exp(-(V + 50)/15))$
Persistent sodium, NaP	$m_{\infty NaP} = (1 + \exp(-(V + 47.1)/3.1))^{-1}$ $h_{\infty NaP} = (1 + \exp((V + 60)/6.5))^{-1}$	$\tau_{mNaP} = 0$ $\tau_{hNaP} = 18000/\cosh((V + 60)/13)$
Potassium rectifier, K	$m_{\infty K} = (1 + \exp(-(V + 28)/4))^{-1}$ $h_K = 1$	$\tau_{mK} = 3.5/\cosh((V + 40)/40)$

Table 2. Maximal conductances of ionic channels (in mS × cm^{-2}) and leakage reversal potentials $\bar{E}_L$ (in mV) in different neuron types

Neuron type	$\bar{g}_{Na}$	$\bar{g}_{NaP}$	$\bar{g}_K$	g_L	$\bar{E}_L$	g_{ChR}	$\bar{E}_{ChR}$
RG-F	25	0.75 (± 0.0375)	2	0.07	−62 (± 0.62)		
RG-E	25	0.75 (± 0.0375)	2	0.07	−56 (± 0.56)		
V2b	10		5	0.1	−62 (± 1.24)	0/0.03*	0
V1-1	10		5	0.1	−62 (± 1.24)	0/0.03*	0
V1	10		5	0.1	−60 (± 1.2)	0/0.03*	0
Ini	10		5	0.1	−47 (± 0.94)		
V3	40		5	0.7	−55 (± 1.65)		
$V0_D$	10		5	0.1	−63 (± 1.26)		
Ini-1	10		5	0.1	−60 (± 1.2)		
V2a	40		5	0.8	−56 (± 1.12)		
$V0_V$	10		5	0.1	−58 (± 1.16)		

*g_{ChR} = 0 in the absence of stimulation and 0.03 mS × cm^{-2} during the applied stimulation.

tonic activity. The values of E_L and initial conditions for each neuron were assigned in advance from the mean values and variances using a random number generator. The assigned values of E_L allowed the model to simulate the drug-evoked fictive locomotion (see Shevtsova *et al.* 2015) and generate locomotor-like rhythmic activity with frequency of 0.4 Hz and approximately equal flexor and extensor phases in control conditions.

Random synaptic connections between the neurons of interacting populations were assigned prior to each simulation based on probability of connection, p, so that, if a population A was assigned to receive an excitatory (or inhibitory) input from a population B, then each neuron in population A received the corresponding synaptic input from each neuron in population B with the probability $p\{A, B\}$. If $p\{A, B\} < 1$, a random number generator was used to define the existence of each synaptic connection; otherwise (if $p\{A, B\} = 1$) each neuron in population A received synaptic input from each neuron of population B. Values of synaptic weights (w_{ji}) between neuron i in the source population and neuron j in the target population were also set using a random number generator based on the average values of these weights $\bar{w}$ and the variances, which were defined as 10% of $\bar{w}$. The average weights and probabilities of connections are specified in the Appendix (Table 3).

All simulations were performed using the custom neural simulation package NSM 4.0 developed at Drexel University by S. N. Markin, I. A. Rybak and N. A. Shevtsova. This simulation package was previously used for the development of several spinal cord models (Rybak *et al.* 2006*a*,*b*, 2013; Zhong *et al.* 2012; Brocard *et al.* 2013; Shevtsova *et al.* 2015). Differential equations were solved using the exponential Euler integration method with a step size of 0.1 ms. A settling period of 20–100 s is allowed in each simulation before data collection.

Results

Analysis of existing experimental data on V1 and V2b neurons and constructing their possible connectivity within the spinal rhythm-generating network

Our approach to the construction of possible connectivity patterns of V1 and V2b neurons was based on several assumptions and requires some preliminary comments. First, our consideration of potential connectivity of these neurons was limited to the level of rhythm-generating circuits. Other levels of neuron interactions in the cord representing pattern formation and reflex circuits were left beyond the scope of the present study (also see Rybak *et al.* 2015). Therefore, and with the account of known

Table 3. Average weights ($\bar{w}$) and probabilities (p) of synaptic connections

Source population	Target populations ($\bar{w}$, p)
i-RG-F	i-RG-F (0.015, $p = 0.1$); i-RG-E (0.005, $p = 0.1$); i-V2b (0.015, $p = 1$);i-V2a (0.01, $p = 1$); i-V3 (0.0075, $p = 1$); i-V0$_D$ (0.005, $p = 1$)
i-RG-E	i-RG-E (0.015, $p = 0.1$); i-RG-F (0.005, $p = 0.1$); i-V1-1 (0.01, $p = 1$)
i-V1-1	i-RG-F (-0.04, $p = 1$)
i-V2b	i-RG-E (-0.08, $p = 1$)
i-V1	i-RG-E (-0.04, $p = 1$); i-Ini (0.8, $p = 1$)
i-Ini	i-RG-F (-0.03, $p = 1$)
i-Ini-1	i-RG-F (-0.01, $p = 1$)
i-V2a	i-V0$_V$ (0.14, $p = 1$)
i-V3	c-RG-F (0.002, $p = 1$)
i-V0$_D$	c-RG-F (-0.01, $p = 1$); c-V1(-0.16, $p = 1$)
i-V0$_V$	c-Ini-1 (0.07, $p = 1$)

Prefixes i- and c- indicate ipsi- and contralateral populations, respectively.

heterogeneity of V1 and V2b populations, we did not consider subpopulations of V1 and V2b neurons that could represent and perform the functions of Ia, Ib, Renshaw and other neuron types not directly involved in the rhythmogenesis. Consequently, terms *V1* and *V2b* below and throughout the paper are used only in relation to subpopulations of V1 and V2b neurons that can be explicitly involved in the interactions between the flexion-related and extension-related rhythm-generating circuits.

Second, we assumed that the neuronal rhythm generator (RG) on each side of the cord consists of two centres (flexor, F or RG-F, and extensor, E or RG-E) that mutually inhibit each other via inhibitory neuron populations, which is generally consistent with the classical half-centre concept (Graham Brown, 1914; Lundberg, 1979; Marder & Calabrese, 1996; Stuart & Hultborn, 2008; McCrea & Rybak, 2008). Furthermore, we followed the concept of asymmetric RG organization that suggested a dominant role of flexor RG centres in generation of locomotor activity (Pearson & Duysens, 1976; Duysens, 1977; Zhong *et al.* 2012; Duysens *et al.* 2013; Machado *et al.* 2015, Rybak *et al.* 2015). Specifically, following our previous models (Zhong *et al.* 2012; Rybak *et al.* 2013; Shevtsova *et al.* 2015; Molkov *et al.* 2015), we suggested that only the flexor RG centres operate in an intrinsic bursting regime while the extensor RG centres if isolated generate tonic or sustained activity and exhibit bursting due to the rhythmic inhibition from the intrinsically bursting ipsilateral flexor RG centres.

The additions to the model begin with the clear experimental evidence that silencing of both V1 and V2b neuron types in the isolated intact cord of neonatal mouse resulted in synchronous flexor and extensor activities, whereas inactivation of either one of these two types on its own did not disturb flexor–extensor alternation (Zhang *et al.* 2014). This statement is illustrated in Fig. 1*Aa* (modified from the similar figure by Zhang *et al.*) showing that both V1 *and* V2b neuron types secure flexor–extensor alternation on each side of the cord. Although this simple schematic representation does not address possible differences in specific roles and connections of these two neuron types, it shows that flexor and extensor RG centres should have mutual excitatory connections to exhibit synchronous activity after silencing of both V1 and V2b inhibitory neuron types (Fig. 1*Ab*).

Then, it was demonstrated that: (1) optogenetic-based photostimulation of V2b neurons in the isolated spinal cord could suppress the extensor-related motor activity without affecting the flexor-related activity, whereas a similar photostimulation of V1 neurons suppressed both flexor and extensor output activities (Britz *et al.* 2015), and (2) selective silencing of V2b neurons in a hemicord (after hemisection) led to synchronization of flexor and extensor activities, whereas silencing of only V1 neurons did not affect flexor–extensor alteration in hemicords (Zhang *et al.* 2014). To satisfy both these features, the schematic representation in Fig. 1*Aa* can be transformed to that in Fig. 1*Ba*. The latter shows that an additional activation of V2b would inhibit the extensor centre, and an additional activation of V1 would inhibit both the flexor and extensor centres. Taking into account our assumption that only the flexor centre is intrinsically bursting, the inactivation of V1 neurons in hemicord should not perturb flexor–extensor alternation provided by the V2b neurons (Fig. 1*Bb*), whereas the inactivation of V2b neurons should lead to the flexor–extensor synchronization (Fig. 1*Bc*).

An important function of V1 neurons, that was not taken into account in Fig. 1*Aa* and *Ba*, is that these neurons are critical for fast locomotor oscillations (Gosgnach *et al.* 2006) and their ablation or silencing slowed down the locomotor activity in the intact cord (Gosgnach *et al.* 2006; Zhang *et al.* 2014) but not in a hemicord, where the locomotor activity had already been slowed

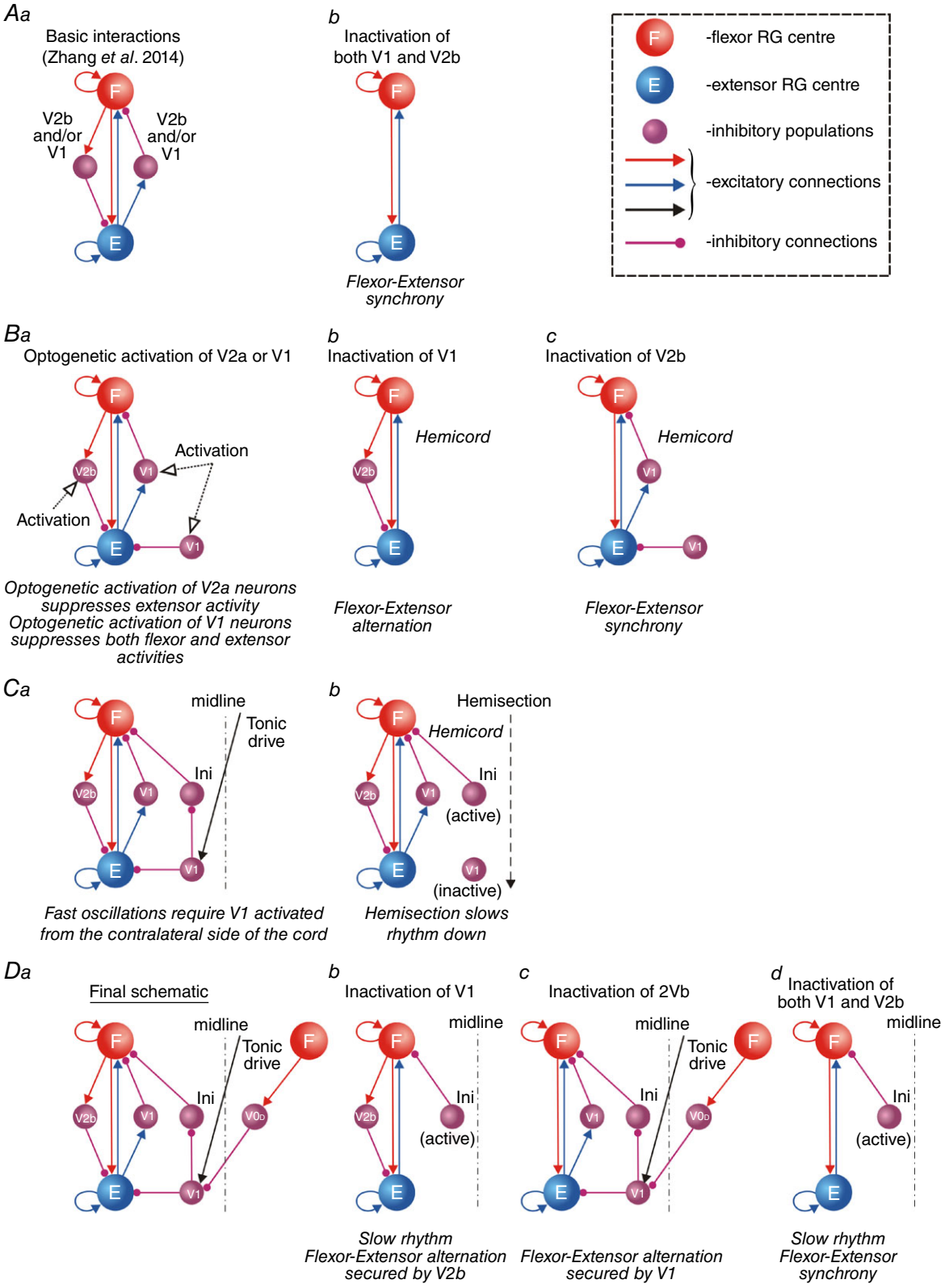

Figure 1. Constructing possible connectivity of V1 and V2b interneurons within the spinal rhythm-generating network
Aa, schematic representation of ipsilateral circuits of the spinal locomotor rhythm generator (RG). The RG on each side of the cord consists of two centres (flexor, F, and extensor, E) mutually inhibiting each other via V1 and/or V2b inhibitory neurons (as suggested by Zhang *et al.* 2014). *Ab*, mutual excitatory connections between the F and E

centres synchronize their activity after inactivation of both V1 and V2b neurons. *Ba*, different role and connectivity of V1 and V2b neurons. Optogenetic photostimulation of V2b neurons in the isolated spinal cord (hollow arrow to the V2b population) suppresses extensor activity while photostimulation of V1 neurons (two hollow arrows to the V1 populations) suppresses both flexor and extensor activities. *Bb*, inactivation of V1 neurons does not affect flexor–extensor alternation in hemicord. *Bc*, inactivation of V2b neurons in hemicord leads to flexor–extensor synchronization. *Ca*, control of fast locomotor oscillations by V1 neurons. Some V1 neurons receive tonic excitation from the contralateral side of the cord and inhibit both the ipsilateral E centre and the Ini population, that disinhibit the ipsilateral F centre, leading to an increase of the locomotor frequency. *Cb*, hemisection makes these V1 neurons silent leading to a slowing down of the locomotor oscillations. *Da*, complimentary roles of V1 and V2b neurons in flexor–extensor interactions. The activity of the V1 population receiving drive from the contralateral side is also negatively modulated by rhythmic inhibition via contralateral commissural $V0_D$ interneurons; this modulation provides additional support of flexor–extensor alternation on the ipsilateral side of the cord. *Db*, after silencing of V1 neurons, flexor–extensor alternation is secured by V2b neurons, but the rhythm slows down because of silencing of V1 neurons. *Dc*, after silencing of V2b neurons, flexor–extensor alternation is supported by V1 neurons receiving contralateral tonic drive and rhythmic inhibition from the contralateral F centre via commissural $V0_D$ neurons. *Dd*, silencing of both V1 and V2b neurons leads to slow synchronized flexor–extensor activity.

down as a result of hemisection (Zhang *et al.* 2014). To satisfy this feature, we suggested that the same V1 neurons (1) activate (disinhibit) the flexor RG centre via the suppression of intermediate inhibitory neurons (Ini) inhibiting this centre and (2) inhibit the extensor RG centre. We also suggested that these V1 neurons are activated by excitatory drive from the contralateral side of the cord. These additional connections transformed the schematic representation in Fig. 1*Ba* to that shown in Fig. 1*Ca*. As shown in this figure, in the intact cord the V1 population should be activated by the contralateral drive and if activated should inhibit the ipsilateral extensor RG centre and activate (disinhibit) the ipsilateral flexor RG centre, hence increasing locomotor frequency. In this case, hemisection would remove the conrtalateral drive to these neurons and hence inactivate these neurons (Fig. 1*Cb*), which should reduce the locomotor frequency.

Yet, the schematic representation shown in Fig. 1*Ca* cannot explain why and how the V1 neurons secure flexor–extensor alternation in the intact cord after silencing V2b neurons (Zhang *et al.* 2014). For this to occur, we suggested that the activity of V1 population receiving excitatory drive from the contralateral cord side is also (negatively) modulated from the contralateral side by the activity of the inhibitory commissural $V0_D$ interneurons that are activated during the contralateral flexion (or ipsilateral extension) (Fig. 1*Da*). This should reduce inhibition of the ipsilateral flexor RG centre and increase inhibition of the ipsilateral extensor RG centre during ipsilateral flexion and hence provide an additional support of flexor–extensor alternation on the ipsilateral side of the cord. We, therefore, suggested that the connectivity patterns of V1 and V2b neurons shown in Fig. 1*Da* can potentially explain most of the experimental results on both selective inactivation and selective stimulation of V1 and V2b neurons in the isolated spinal cord. Specifically, silencing of V1 neurons (Fig. 1*Db*) should slow down locomotor oscillations (as in Fig. 1*Cb*) but maintain flexor–extensor alternation secured by V2b neurons; inactivation of V2b neurons (Fig. 1*Dc*) also should not disturb flexor–extensor alternation, which would be secured by the modulated activity of V1 neurons; and only inactivation of both these neuron types (Fig. 1*Dd*) would lead to flexor–extensor synchronization.

Incorporating V1 and V2b neuron populations in a larger computational model of rhythm-generating spinal circuits simulating left–right interactions in the spinal cord

In order to further evaluate the connectivity patterns of V1 and V2b neurons proposed in Fig. 1*Da*, populations of these neurons with all their suggested connections were incorporated in our previous model simulating bilaterally interacting rhythm-generating spinal circuits (Shevtsova *et al.* 2015, Model 1). The schematic representation of the final integrated model is shown in Fig. 2. Similar to the preceding model, this model contains two (left and right) rhythm generators (l-RG and r-RG, respectively), each of which includes two excitatory neural populations representing flexor (RG-F) and extensor (RG-E) centres, respectively. Also, consistent with the Model 1 of Shevtsova *et al.* (2015), the bilateral interactions between the left and right RGs are mediated by three types of commissural pathways involving three types of commissural interneurons (CINs) (Fig. 2). Two of these pathways provide mutual inhibition between left and right RG-F centres, promoting left–right alternation: one mediated by the inhibitory $V0_D$ CINs (left, l-$V0_D$, and right, r-$V0_D$), and the other representing a chain of the V2a neurons, the excitatory $V0_V$ CINs, and the inhibitory Ini-1 interneurons (all are either left, l-, or right, r-). The third commissural pathway type is mediated by the left and right excitatory V3 CINs (l-V3 and r-V3) and promotes left–right synchronization.

Similar to the preceding model, both flexor and extensor RG centres represent populations of excitatory neurons with intrinsically bursting properties defined by the persistent (slowly inactivating) sodium currents (I_{NaP}) in each neuron (Shevtsova *et al.* 2015). These intrinsic

bursting properties are state dependent, so that with increase of neuronal excitability, each neuron changes the state of activity from silence to rhythmic bursting with burst frequency increasing with the excitability, and then to sustained tonic activity. However, as mentioned above, we have implemented an asymmetric RG organization, in which only the flexor centres (l-RG-F and r-RG-F) operate in the bursting regime, whereas the extensor centres (l-RG-E and r-RG-E) if isolated operate in the mode of tonic activity and exhibit bursting because of the rhythmic inhibition from the corresponding bursting flexor RG centres (the detailing discussion of this issue can be found in Shevtsova *et al.* 2015).

To incorporate V1 and V2b populations with their connections shown in Fig. 1*Da*, we first included mutual excitatory connections between the RG-F and RG-E centres on each side of the cord (Fig. 2). Then we included V2b populations, mediating the flexor–extensor inhibition on each side, and V1 (V1-1) populations mediating extensor–flexor inhibition (Figs 1*Da* and 2). We then also incorporated the second V1 (V1) populations that provided direct inhibition of the RG-E centre and disinhibition of the RG-F centre on each side. The latter operated via intermediate inhibitory neurons (l-Ini and r-Ini), which were set to be tonically active at rest (Figs 1*Da* and 2). Finally, similar to Fig. 1*Da*, these V1 populations received constant excitatory drive and phasic inhibitory input from $V0_D$ CINs, both from the contralateral cord side of the cord (Fig. 2).

All modifications made to incorporate V1 and V2b populations with their connectivity patterns did not perturb the ability of the integrated model to reproduce the results described in the preceding paper, including the speed-dependent contributions of $V0_D$ and $V0_V$ CINs and V2a interneurons to left–right alternation in the intact cord, switching the locomotor pattern from the left–right alternating walking-like activity to the left–right synchronous hopping-like pattern after removal of different CINs ($V0_D$, $V0_V$, or both) and V2a neurons, and speed-dependent asymmetric changes of flexor and extensor phase durations (Shevtsova *et al.* 2015). The use of the model for simulating the experiments with selective silencing or activation of V1 and V2b neurons is considered below.

Model performance: simulation of V1 and V2b neurons inactivation and stimulation

Performance of the model: rhythm generation in the intact cord *vs.* hemicord. It is known that hemisection significantly reduces the frequency of locomotor oscillations (by at least 2–3 times), while maintaining left–right and flexor–extensor alternation in the activity recorded from ventral roots L2 (flexion-related) and

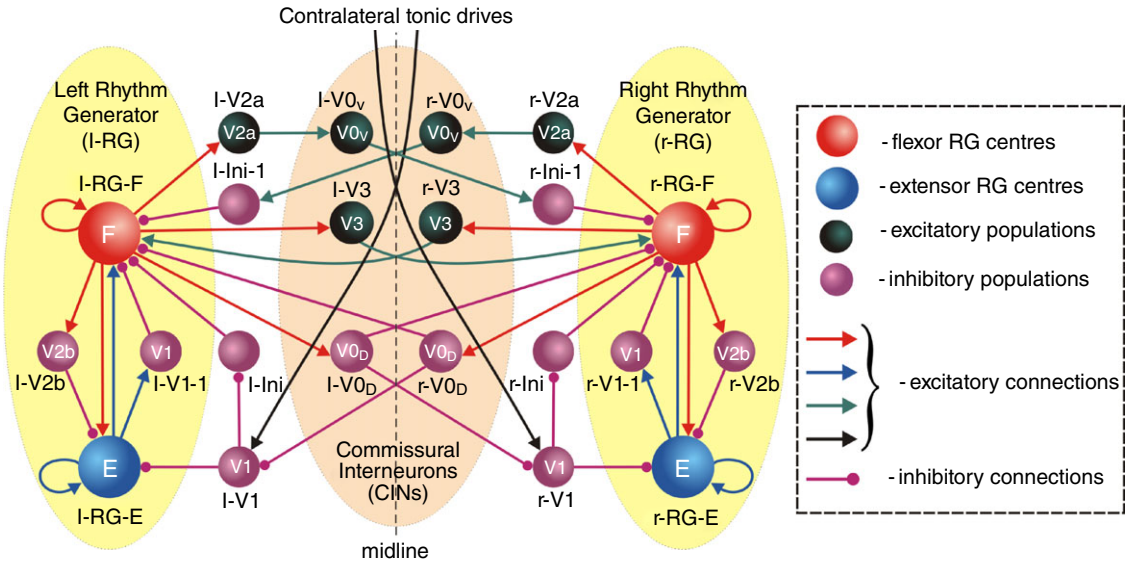

Figure 2. Model architecture
The rhythm generator (RG) on each side of the cord includes the flexor and extensor rhythm generating centres (left (l-) and right (r-) RG-F and RG-E, respectively) mutually exciting each other and reciprocally interacting via the inhibitory V2b and V1-1 populations (l-V2b and r-V2b, and l-V1-1 and r-V1-1, respectively). The left and right RGs interact via commissural interneuron (CIN) populations: l-V3, r-V3, l-$V0_D$, r-$V0_D$, l-$V0_V$, and r-$V0_V$ (see Shevtsova *et al.* 2015). The additional population of V1 (l-V1 and r-V1) neurons on each side is involved in flexor–extensor and left–right interactions and participates in regulating locomotor frequency (via the inhibitory l-Ini1 and r-Ini1 populations) and in securing ipsilateral flexor–extensor alternation by rhythmic inhibition of the ipsilateral RG-E population. The l-V1 and r-V1 populations receive tonic contralateral drive and rhythmic inhibition from the contralateral RG-F population via the inhibitory $V0_D$ CIN population.

L5 (extensor-related) (Cazalets *et al.* 1995; Kjaerulff & Kiehn, 1996; Kiehn & Kjaerulff, 1998; Bertrand & Cazalets, 2002; Zhong *et al.* 2012; Zhang *et al.* 2014). Our integrated model is able to generate rhythmic busting activity in a wide range of frequencies showing alternating left–right and flexor–extensor activity (see an example in Fig. 3*Aa*). Simulated hemisection removed the contralateral excitatory drive to V1 populations (Fig. 2) making these populations silent. This caused disinhibition of both the RG-E centre and the inhibitory Ini population in each hemicord. As a result, the Ini population increased inhibition of the RG-F centre. Both the increased inhibition of the RG-F centre and disinhibition of the RG-E centre led to the slowing down of the locomotor oscillations generated in a simulated hemicord (see Fig. 3*Ca*). This reduction of oscillation frequency fits to the reduction in the locomotor frequency following hemisection in the isolated spinal cord (compare Fig. 3*Aa* and *Ca* with Fig. 3*Ba* and *Da*).

Effects of inactivation of V1 and V2b neurons. Similar to the hemisection, selective inactivation of V1 neurons from the intact cord model slowed down the locomotor rhythm while maintaining flexor–extensor alternation provided by V2b neurons (Fig. 3*Ab*). Inactivation of the V1 population did not produce visible effects on the simulated hemicord activity (Fig. 3*Cb*), since the rhythm was already slowed down by simulated hemisection (Fig. 3*Ca*). These simulation results generally fit to the experimental data on the isolated mouse cord following selective inactivation of V1 neurons in the intact cord (Fig. 3*Bb*) and hemicord (Fig. 3*Db*).

Selective inactivation of V2b neurons did not cause visible changes in the intact cord model (Fig. 3*Ac*), but led to flexor–extensor synchronization in the hemicord model (Fig. 3*Cc*). The results of these simulations appear to be consistent with the experimental data on the effects of selective inactivation V2b neurons in the intact cord (compare Fig. 3*Ac* with Fig. 3*Bc*) and hemicord (compare Fig. 3*Cc* with Fig. 3*Dc*).

Finally inactivation of both V1 and V2b neurons in the model led to flexor–extensor synchronization in both the intact cord (Fig. 3*Ad*) and the hemicord (Fig. 3*Cd*) models, which also corresponds to the existing experimental data (Fig. 3*Bd* and *Dd*).

Effects of V1 and V2b neuron activation. To investigate the specific roles of V2a and V1 neurons in spinal cord rhythmic activity, Britz *et al.* (2015) used selective optogenetic activation of these neurons in the isolated mouse spinal cord. To simulate the effect of photostimulation, we selectively activated the particular neuron types in our model by increasing the channelrhodopsin leak conductances (g_{ChR}, see Methods and Appendix). In our model, V2b neurons provide inhibition of the extensor centres (RG-E) on both sides of the cord (see Fig. 2) with no direct influence on the flexor centres (RG-F). Therefore, an additional activation of these neurons suppressed extensor activity (RG-E) without an obvious effect on flexor activity (Fig. 4*Aa*). These results of simulation are consistent with the effects of selective photostimulation of V2b neurons in the isolated spinal cord (Fig. 4*Ba*).

In contrast to V2b neurons, the V1 populations in our model inhibit both the RG-E and RG-F centres (V1 and V1-1 populations, see Fig. 2). Therefore, selective activation of these populations suppressed both flexor and extensor activities (Fig. 4*Ab*), which is also consistent with experimental studies (Fig. 4*bc*).

Discussion

Although neural circuits in mammalian spinal cord including the hypothetical CPGs controlling locomotion have been studied for more than 100 years starting with the classical works of Graham Brown (1911, 1914), their organization remains mainly unknown (Grillner, 2006; Kiehn, 2006). Significant progress has been recently made due to the novel molecular-genetic and optogenetic approaches. Several classes of spinal neurons have been identified based on transcription factor expression and other developmental/molecular properties, including the so-called V0 ($V0_D$ and $V0_V$ subtypes), V1, V2a, V2b, V3, Hb9 and Shox2 interneurons (Lanuza *et al.* 2004; Goulding, 2009; Kiehn, 2011, 2016; Dougherty *et al.* 2013; Catela *et al.* 2015; Lu *et al.* 2015). However, many of these classes have multiple subclasses. Moreover, the exact functions of these neurons have not been clearly established and their connections remain mostly unknown. Since neurons that are directly involved in rhythm-generation in the mammalian spinal cord remain unknown and because of a general lack of recording from most of these neurons, the functional roles of these neurons and their potential connections are usually suggested from the analysis of the changes in the output motor activity following silencing or optogenetic stimulation/suppression of each neuron type or from the analysis of motor activity generated in mutants lacking each neuron type. The proposed function of these neurons and their connectivities can then be validated using computational modelling. This approach was previously used in studying the role of CINs of $V0_D$ and $V0_V$ types involved in the left–right coordination of neuronal activity in the mouse spinal cord *in vitro* (Talpalar *et al.* 2013; Molkov *et al.* 2015; Shevtsova *et al.* 2015; Rybak *et al.* 2015), as well as in the speed-dependent gait expression in mice *in vivo* (Bellarita & Kiehn, 2015). A similar studies of the role of ipsilaterally projecting, inhibitory interneurons of V1 and V2b types *in vitro* and *in vivo* (Zhang *et al.* 2014; Britz *et al.* 2015). The

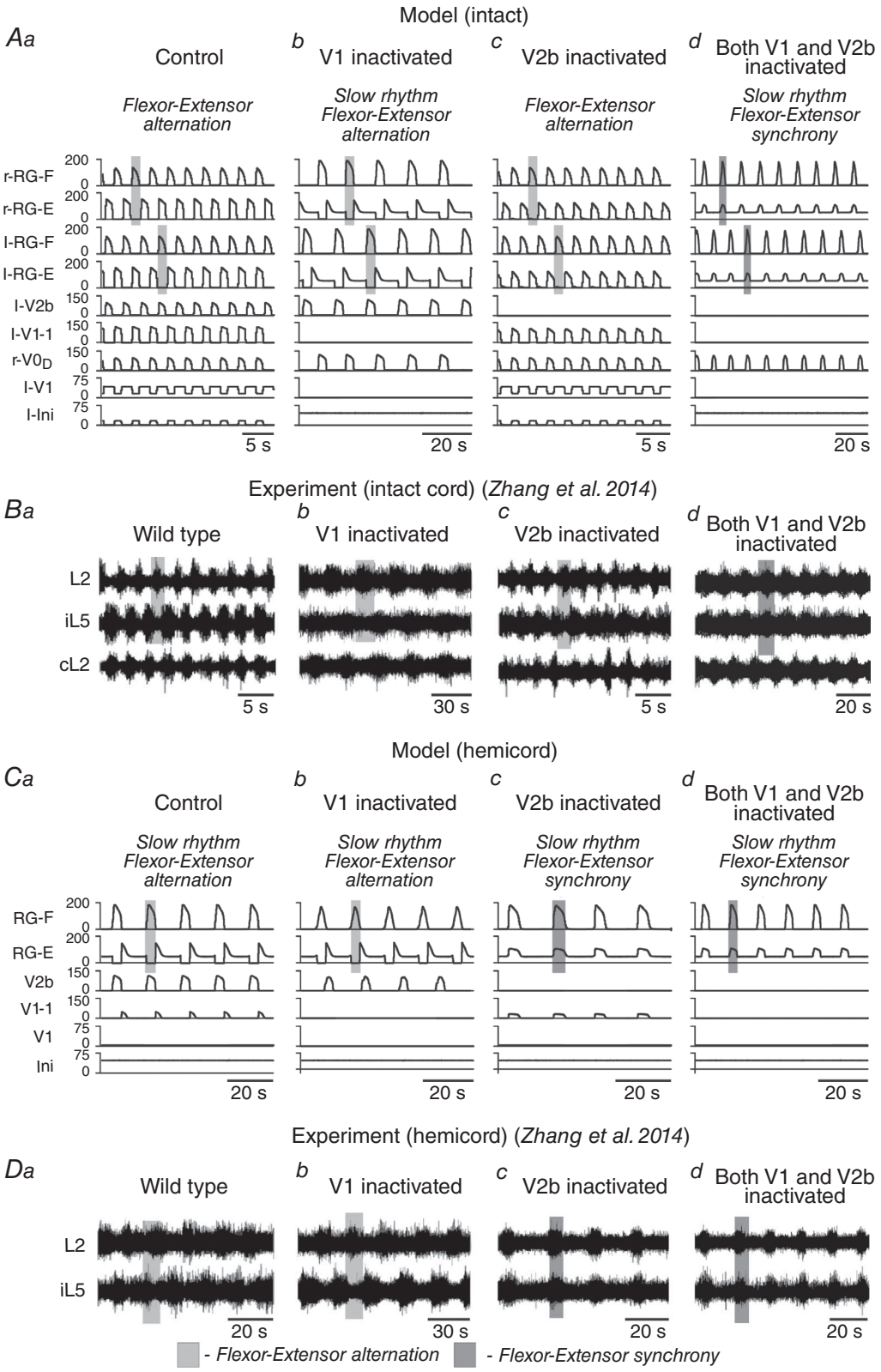

Figure 3. Effects of selective inactivation of V1 and V2b neurons in the intact cord and hemicord: comparison of simulations with experimental data
Aa–d, integrated activities of four RG centres (l-RG-E, l-RG-F, r-RG-F and r-RG-E) and interneuron populations involved in coordination of flexor–extensor activity on the left side of the cord for the intact model (l-V2b, l-V1-1, r-$V0_D$, l-V1 and l-Ini1): *a*, control; *b*, after selective inactivation of V1 populations; *c*, after selective inactivation of

V2b populations; *d*, after inactivation of both V1 and V2b populations. *Ba–d*, corresponding experimental results from the Zhang *et al.* (2014) study (their Figs 4*A*, 1*A*, 4*B* and 5*A*, respectively), reproduced with permission. *Ca–d*, integrated activities of ipsilateral RG populations (RG-F and RG-E) and interneuron populations shaping the flexor–extensor activity after simulated hemisection (V2b, V1-1, V1, and Ini): *a*, control; *b*, after selective inactivation of V1 populations; *c*, after selective inactivation of V2b population; *d*, after inactivation of both V1 and V2b populations. *Da–d*, corresponding experimental results from Zhang *et al.* (2014) study (Figs. 4*C*, 1*B*, 4*D* and S3, respectively) reproduced with permission. In *Aa–d* and *Ca–d*, activities of all populations are shown as average histograms of neuron activity [spikes/(neuron × s), bin = 50 ms].

latter studies used selective silencing and optogenetic activation of V1 and V2b neurons to investigate their specific roles in flexor–extensor alternation of neuronal activity in the spinal cord. Here, we extended our previous model of spinal circuits (Shevtsova *et al.* 2015) by incorporating populations of V1 and V2b neurons and used the extended model to propose the connectivity patterns of these neurons allowing the model to reproduce the results of the above experimental studies.

Both V1 and V2b neurons are heterogeneous neural populations and each includes multiple different subpopulations representing such functional neuron types as Renshaw cells (V1), Ia interneurons that mediate reciprocal inhibition between antagonist motoneurons (both V1 and V2b), Ib interneurons involved in non-reciprocal inhibition of motoneurons (V2b), as well as other as yet unidentified inhibitory cell types (Sapir *et al.* 2004; Alvarez approach was also used in the experimental *et al.* 2005; Zhang *et al.* 2014). Therefore silencing/removal or extra activation of all V1 or all V2b cells can disturb flexor–extensor relationships at several levels of the spinal cord network, including the pattern formation and reflex circuits and motoneurons (e.g. via Ia, Ib, or Renshaw cells), and not necessarily at the level of rhythm-generating circuits involved in locomotion. The main source of evoked disturbances is difficult to establish, especially if to have only recordings from ventral roots representing the common motor outputs of the spinal circuitry. Silencing of V1 and V2b cells performing functions of Ia, Ib or Renshaw cells could affect the intensity of motoneuron

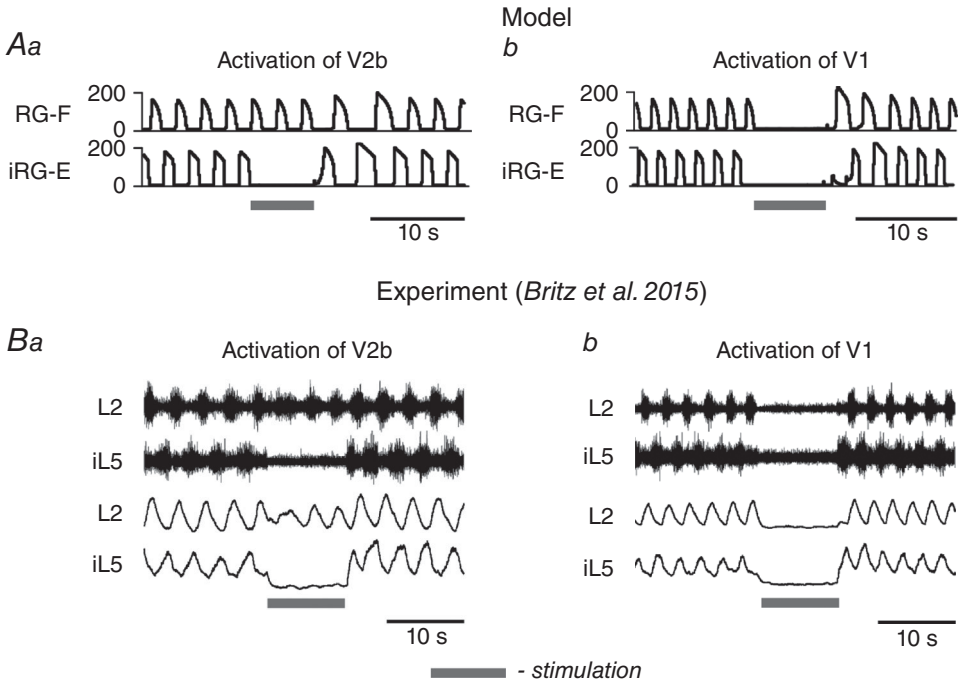

Figure 4. Effects of selective activation of V2b and V1 neurons: comparison of simulations with experimental data
Aa, activation of V2b neurons in the model suppressed the extensor activity (RG-E) with minimal effect on flexor activity (RG-F). *Ab*, activation of V1 neurons in the model suppressed both flexor and extensor RG activity. *Ba*, effect of optogenetic stimulation of V2b neurons during drug-induced locomotion in the isolated mouse spinal cord: suppression of activity in the extensor-related (L5) root but maintenance of rhythmic activity in the flexor-related root (L2). *Bb*, effect of optogenetic stimulation of V1 neurons: suppression of activity in both the flexor-related (L2) the extensor-related (L5) roots. Experimental recordings in *Ba* and *Bb* are from Britz *et al.* (2015), Fig. 7*C* and *E*). Grey bars show time intervals when stimulation was applied.

activities. Yet our major focus was on the potential effects on the rhythm-generating circuits, which we tried to model in this study. Therefore, we were mostly interested in effects such as changes in the locomotor frequency or occurrence of flexor–extensor synchronization (which were supposedly connected with disturbances at the RG level) rather than in the demonstrated hyperactivation of flexor or extensor muscles (Britz *et al.* 2015) or other changes that could happen at the reflex circuit or motoneuron levels.

Rhythm generator: asymmetric organization

Most of earlier bipartite models assumed a symmetric organization of flexor and extensor RG centres and their interactions. An asymmetric, flexor-dominated organization was initially proposed by Pearson and Duysens (Pearson & Duysens, 1976; Duysens, 1977) and analysed and discussed in later studies (see Zhong *et al.* 2012; Duysens *et al.* 2013; Machado *et al.* 2015). The concept of asymmetric organization was implicitly supported by the analysis of deletions (missing flexor or extensor bursts) during drug-evoked fictive locomotion in the isolated spinal cord preparations (Zhong *et al.* 2012). This analysis revealed only two types of deletions: missing bursts in the activity of flexor-dominated ventral roots (L2) were always accompanied by a sustained activity in the ipsilateral extensor-dominated roots (L5), whereas missing extensor bursts occurred without obvious disturbances of the flexor rhythmic activity. Also, the analysis of changes in the duration of flexor and extensor phases with an increase in the oscillation frequency during drug-evoked fictive locomotion in the isolated spinal cord showed that the changes in the duration of the flexor phase were much less than changes in the duration of the extensor phase (Talpalar *et al.* 2013; Shevtsova *et al.* 2015), which also fit with similar phase changes in cats *in vivo* (Halbertsma, 1983; Frigon & Gossard, 2009). This evidence led to the suggestion, which was accepted in this study, that the extensor RG centre of the spinal rhythm generator operates in a regime of sustained activity and hence does not generate rhythmic activity if isolated, but exhibits rhythmic bursting due to inhibition from the corresponding flexor RG centre that generates population rhythmic activity due to the intrinsic neuron properties and neuronal synchronization within the RG centres (Shevtsova *et al.* 2015; Rybak *et al.* 2015). The intrinsic neuron properties involved in this rhythmogenesis can affect network and system performance. However, these properties remain mainly unknown. Previous experimental and modelling studies have suggested that the persistent (slowly inactivating) sodium current may play an important role in the spinal cord rhythm generation (Rybak *et al.* 2006*a*,*b*; 2013; McCrea & Rybak, 2007; Tazerart *et al.*, 2007, 2008; Zhong *et al.* 2007, 2012; Ziskind-Conhaim *et al.* 2008; Brocard *et al.* 2010, 2013; Shevtsova *et al.* 2015), which was implemented in the current model.

The potential roles of V1 neurons and their connectivity

The important function of V1 neurons, or at least one of their subpopulations, is to speed up the locomotor oscillations (Gosgnach *et al.* 2006), so that removal or silencing these neurons slowed down the locomotor oscillations (Gosgnach *et al.* 2006; Zhang *et al.* 2014; see Fig. 3*Bb*). The question here is how silencing of inhibitory neurons could actually cause an increase in oscillatory frequency. One reasonable explanation for that could be based on a suggestion that these neurons disinhibit rhythm-generating circuits (Fig. 1*Ca*), which was implemented in our model (Fig. 2). It is also interesting, that (a) slowing the rhythm after silencing of V1 neurons was similar to that following hemisection (compare Fig. 3*Bb* with Fig. 3*Da*) and (b) silencing of these neurons did not produce obvious changes in the locomotor rhythm in a hemicord, i.e. after hemisection (compare Fig. 3*Da* with Fig. 3*Db*). To explain this, we proposed that there are subpopulations of V1 neurons that are activated from contralateral side of the cord and speed up the rhythm via disinhibition of ipsilateral rhythm-generating circuits. The contralateral tonic activation of these neurons could come from some tonically active commissural neurons. Such hypothetical V1 populations were incorporated in our model (Fig. 2, left and right V1 populations) and allowed the model to reproduce the above experimental data (see Fig. 3*Aa*,*b* and *Ca*,*b* and compare with Fig. 3*Ba*,*b* and *Da*,*b*, respectively). This suggestion awaits experimental testing.

Furthermore, it was shown that V1 neurons secured the flexor–extensor alternation after silencing V2b neurons in the intact cord, but not in a hemicord (Zhang *et al.* 2014; Fig. 3*Bc* and 3*Dc*). With the account of this, the above proposal should be extended by a suggestion that these V1 neurons are not only activated from the contralateral side, but their activity is (negatively) modulated by the contralateral rhythmic flexor activity. The simplest way to explain such modulation would be to suggest that the V1 population is inhibited by contralateral inhibitory CINs, such as $V0_D$ (Fig. 1*Da*). This suggestion was implemented in our model (Fig. 2) and allowed it to reproduce experimental data related to inactivation of V2b neurons *vs.* inactivation of both V2b and V1 neurons (see Fig. 3*Ac*,*d* and *Cc*,*d* and compare with Fig. 3*Bc*,*d* and *Dc*,*d* respectively). We therefore consider the inhibition of some V1 neurons by the contralateral $V0_D$ CINs as our theoretical predictions.

In any case, our analysis and simulations suggest that V1 neurons play a critical role in the interactions between the

spinal circuits responsible for flexor–extensor alternation and those responsible for left–right coordination.

It was also shown that an optogenetic stimulation of V1 neurons in the isolated mouse spinal cord during drug-induced locomotion suppressed rhythmic activity on both flexor-related (L2) and extensor related (L5) roots (Britz *et al.* 2015; Fig. 4*Bb*). In our model, this effect of V1 photostimulation was reproduced (see Fig. 4*Ab*) due to special organization of connections of two populations of V1 neurons inhibiting both the flexor and extensor RG-centres (Figs 1*Ca* and 2). However, the same effect can be also produced at the reflex and motoneuron levels by stimulation of V1 cells performing the functions of Renshaw cell or Ia neurons (Britz *et al.* 2015). The current data are not sufficient to judge which of the two suggestions is more plausible.

The potential roles of V2b neurons and their connectivity

Experimental data of Zhang *et al.* (2014) suggest that V2b neurons are involved in flexor–extensor alternation in the intact cord together with V1 neurons and are solely responsible for flexor–extensor alternation in hemicords (Fig. 3*Bc,d* and *Dc,d*). Based on our simulations, we suggested that V2b neurons mediate inhibition of the extensor RG centre by the flexor RG centre (Fig. 2). This suggestion allowed us to reproduce experimental data of Zhang *et al.* concerning silencing of these neurons (Fig. 3*Ac,d* and *Cc,d*). The other possibility could be that these neurons are involved in mediating the mutual inhibition between the flexor and extensor RG centres in both directions, from flexor to extensor RG centres and from extensor to flexor RG centres (see Rybak *et al.* 2015).

Photostimulation of V2b neurons in the isolated spinal cord led to the suppression of only extensor-related motor activity (L5) leaving the flexor motor activity (L2) not affected (Britz *et al.* 2015; see Fig. 4*Ba*), which was reproduced by our simulations (Fig. 4*Aa*), supporting the suggested role of these neurons in the flexor-to-extensor inhibition. However, similar to that in the case of V1 neurons, additional studies are required to establish where in the spinal network this suppression takes place.

Conclusions

In this theoretical and computational study we made an attempt to analyse the existing experimental data and use this analysis to propose possible roles of genetically identified V1 and V2b neurons in the spinal network and their connections. We were able to incorporate populations of these neurons in a larger model of rhythm-generating circuits and to use the integrated model to reproduce multiple experimental data concerning the effect of selective silencing and activations of these neuron types.

Combining these results with the results of our previous paper (Shevtsova *et al.* 2015) we propose a plausible architecture of spinal circuits that includes most of the genetically identified neurons, including $V0_D$, $V0_V$, V1, V2a, V2b and V3 (Fig. 2). This network architecture allowed the model to reproduce multiple experimental data from different laboratories concerning the effects of various genetic manipulations (ablation, inactivation, photostimulation) with these neuron types. The specific function of these neurons and their possible connections suggested by our models await experimental testing and validation.

Appendix

All neurons are simulated in Hodgkin–Huxley style as single-compartment models. The membrane potential, V, in neurons of the left and right RG-E and RG-F populations is described by the following differential equation

$$C \times \frac{dV}{dt} = -I_{Na} - I_{NaP} - I_K - I_L - I_{SynE} - I_{SynI}, \quad (1)$$

where C is the membrane capacitance and t is time.

In all other populations, the neuronal membrane potential is described as follows:

$$C \times \frac{dV}{dt} = -I_{Na} - I_K - I_L - I_{SynE} - I_{SynI}\ (-I_{ChR}). \quad (2)$$

The ionic currents in Eqns (1) and (2) are described as follows:

$$\begin{aligned} I_{Na} &= \bar{g}_{Na} \times m_{Na}^3 \times h_{Na} \times (V - E_{Na}), \\ I_{NaP} &= \bar{g}_{NaP} \times m_{NaP} \times h_{NaP} \times (V - E_{Na}), \\ I_K &= \bar{g}_K \times m_K^4 \times (V - E_K), \\ I_L &= g_L \times (V - E_L), \\ I_{ChR} &= g_{ChR} \times (V - E_{ChR}), \end{aligned} \quad (3)$$

where I_{Na} is the fast Na^+ current with maximal conductance $\bar{g}_{Na}$; I_{NaP} is the persistent (slowly inactivating) Na^+ current with maximal conductance $\bar{g}_{NaP}$ (present only in RG neurons); I_K is the delayed-rectifier K^+ current with maximal conductance $\bar{g}_K$; I_L is the leakage current with constant conductance g_L; and I_{ChR} is the channelrhodopsin current with the conductance g_{ChR} (present only in V1 and V2a neurons). E_{Na}, E_K, E_L, and E_{ChR} are the reversal potentials for Na^+, K^+, leakage and channelrhodopsin currents, respectively; variables m and h with indexes indicating ionic currents are the activation and inactivation variables of the corresponding ionic channels.

Activation m and inactivation h of voltage-dependent ionic channels (e.g. Na, NaP, and K) in Eqn (3) are described by the following differential equations:

$$\begin{aligned} \tau_{mi}(V) \times \frac{\mathrm{d}}{\mathrm{d}t} m_i &= m_{\infty i}(V) - m_i, \\ \tau_{hi}(V) \times \frac{\mathrm{d}}{\mathrm{d}t} h_i &= h_{\infty i}(V) - h_i, \end{aligned} \tag{4}$$

where $m_{\infty i}(V)$ and $h_{\infty i}(V)$ define the voltage-dependent steady-state activation and inactivation of the channel i, respectively, and $\tau_{mi}(V)$ and $\tau_{hi}(V)$ define the corresponding time constants. Activation of the sodium channels is considered to be instantaneous ($\tau_{m\mathrm{Na}} = \tau_{m\mathrm{NaP}} = 0$). The expressions for channel kinetics, maximal conductances and E_{L} values are given in Tables 1 and 2, respectively.

The synaptic excitatory (I_{SynE} with conductance g_{SynE} and reversal potential E_{SynE}) and inhibitory (I_{SynI} with conductance g_{SynI} and reversal potential E_{SynI}) currents are described as follows:

$$\begin{aligned} I_{\mathrm{SynE}} &= g_{\mathrm{SynE}} \times (V - E_{\mathrm{SynE}}), \\ I_{\mathrm{SynI}} &= g_{\mathrm{SynI}} \times (V - E_{\mathrm{SynI}}), \end{aligned} \tag{5}$$

where g_{SynE} and g_{SynI} are equal to zero at rest and are activated by the excitatory or inhibitory inputs, respectively:

$$\begin{aligned} g_{\mathrm{SynE}i}(t) &= \bar{g}_{\mathrm{E}} \times \sum_j S\{w_{ji}\} \times \sum_{t_{kj}<t} \exp(-(t - t_{kj})/\tau_{\mathrm{SynE}}), \\ g_{\mathrm{SynI}i}(t) &= \bar{g}_{\mathrm{I}} \times \sum_j S\{-w_{ji}\} \times \sum_{t_{kj}<t} \exp(-(t - t_{kj})/\tau_{\mathrm{SynI}}), \end{aligned} \tag{6}$$

where $S\{x\} = x$, if $x \geq 0$, and 0 if $x < 0$. Each spike arriving to neuron i in a target population from neuron j in a source population at time t_{kj} increases the excitatory synaptic conductance by $\bar{g}_{\mathrm{E}} \times w_{ij}$ if the synaptic weight $w_{ji} > 0$, or increases the inhibitory synaptic conductance by $-\bar{g}_{\mathrm{E}} \times w_{ij}$ if the synaptic weight $w_{ji} < 0$. $\bar{g}_{\mathrm{E}}$ and $\bar{g}_{\mathrm{I}}$ define an increase in the excitatory or inhibitory synaptic conductance, respectively, produced by one arriving spike at $|w_{ji}| = 1$. τ_{SynE} and τ_{SynI} are the decay time constants for g_{SynE} and g_{SynI}, respectively. Average weights ($\bar{w}$) and probabilities (p) of synaptic connections are specified in Table 3.

The following general neuronal parameters were assigned:

$C = 1\ \mu\mathrm{F} \times \mathrm{cm}^{-2}$, $E_{\mathrm{Na}} = 55$ mV, $E_{\mathrm{K}} = -80$ mV, $E_{\mathrm{ChR}} = 0$ mV, $E_{\mathrm{SynE}} = -10$ mV, $E_{\mathrm{SynI}} = -70$ mV, $\bar{g}_{\mathrm{E}} = \bar{g}_{\mathrm{I}} = 0.05\ \mathrm{mS} \times \mathrm{cm}^{-2}$, $\tau_{\mathrm{SynE}} = \tau_{\mathrm{SynI}} = 5$ ms.

References

Alvarez FJ, Jonas PC, Sapir T, Hartley R, Berrocal MC, Geiman EJ, Todd AJ & Goulding M (2005). Postnatal phenotype and localization of spinal cord V1 derived interneurons. *J Comp Neurology* **493**, 177–192.

Bellarita C & Kiehn O (2015). Phenotypic characterization of speed-associated gait changes in mice reveals modular organization of locomotor networks. *Curr Biol* **25**, 1426–1436.

Bertrand S & Cazalets JR (2002). The respective contribution of lumbar segments to the generation of locomotion in the isolated spinal cord of newborn rat. *Eur J Neurosci* **16**, 1741–1750.

Britz O, Zhang J, Grossmann KS, Dyck J, Kim JC, Dymecki S, Gosgnach S & Goulding M (2015). A genetically defined asymmetry underlies the inhibitory control of flexor-extensor locomotor movements. *Elife* **4**, e04718.

Brocard F, Shevtsova NA, Bouhadfane M, Tazerart S, Heinemann U, Rybak IA & Vinay L (2013). Activity-dependent changes in extracellular Ca^{2+} and K^{+} reveal pacemakers in the spinal locomotor-related network. *Neuron* **77**, 1047–1054.

Brocard F, Tazerart S & Vinay L (2010). Do pacemakers drive the central pattern generator for locomotion in mammals? *Neuroscientist* **16**, 139–155.

Catela C, Shin MM & Dasen JS (2015). Assembly and function of spinal circuits for motor control. *Annu Rev Cell Dev Biol* **31**, 669–698.

Cazalets JR, Borde M & Clarac F (1995). Localization and organization of the central pattern generator for hindlimb locomotion in newborn rat. *J Neurosci* **15**, 4943–4951.

Dougherty KJ, Zagoraiou L, Satoh D, Rozani I, Doobar S, Arber S, Jessell TM & Kiehn O (2013). Locomotor rhythm generation linked to the output of spinal shox2 excitatory interneurons. *Neuron* **80**, 920–933.

Duysens J (1977). Reflex control of locomotion as revealed by stimulation of cutaneous afferents in spontaneously walking premammillary cats. *J Neurophysiol* **40**, 737–751.

Duysens J, De Groote F & Jonkers I (2013). The flexion synergy, mother of all synergies and father of new models of gait. *Front Comput Neurosci* **7**, 14.

Frigon A & Gossard JP (2009). Asymmetric control of cycle period by the spinal locomotor rhythm generator in the adult cat. *J Physiol* **587**, 4617–4628.

Gosgnach S, Lanuza GM, Butt SJ, Saueressig H, Zhang Y, Velasquez T, Riethmacher D, Callaway EM, Kiehn O & Goulding M (2006). V1 spinal neurons regulate the speed of vertebrate locomotor outputs. *Nature* **440**, 215–219.

Goulding M (2009). Circuits controlling vertebrate locomotion: moving in a new direction. *Nat Rev Neurosci* **10**, 507–518.

Goulding M, Bourane S, Garcia-Campmany L, Dalet A & Koch S (2014). Inhibition downunder: an update from the spinal cord. *Curr Opin Neurobiol* **26**, 161–166.

Graham Brown T (1911). The intrinsic factors in the act of progression in the mammal. *Proc R Soc Lond B Biol Sci* **84**, 308–319.

Graham Brown T (1914). On the nature of the fundamental activity of the nervous centres; together with an analysis of the conditioning of rhythmic activity in progression, and a theory of the evolution of function in the nervous system. *J Physiol* **48**, 18–46.

Grillner S (2006). Biological pattern generation: the cellular and computational logic of networks in motion. *Neuron* **52**, 751–766.

Halbertsma JM (1983). The stride cycle of the cat: the modelling of locomotion by computerized analysis of automatic recordings. *Acta Physiol Scand Suppl* **521**, 1–75.

Kiehn O (2006). Locomotor circuits in the mammalian spinal cord. *Annu Rev Neurosci* **29**, 279–306.

Kiehn O (2011). Development and functional organization of spinal locomotor circuits. *Curr Opin Neurobiol* **21**, 100–109.

Kiehn O (2016). Decoding the organization of spinal circuits that control locomotion. *Nature Rev Neurosci* **17**, 224–238.

Kiehn O & Kjäerulff O (1998). Distribution of central pattern generators for rhythmic motor outputs in the spinal cord of limbed vertebrates. *Ann NY Acad Sci* **860**, 110–129.

Kjäerulff O & Kiehn O (1996). Distribution of networks generating and coordinating locomotor activity in the neonatal rat spinal cord *in vitro*: a lesion study. *J Neurosci* **16**, 5777–5794.

Lanuza GM, Gosgnach S, Pierani A, Jessell TM & Goulding M (2004). Genetic identification of spinal interneurons that coordinate left-right locomotor activity necessary for walking movements. *Neuron* **42**, 375–386.

Lu DC, Niu T & Alaynick WA (2015). Molecular and cellular development of spinal cord locomotor circuitry. *Front Mol Neurosci* **8**, 25.

Lundberg A (1979). Multisensory control of spinal reflex pathways. *Prog Brain Res* **50**, 11–28.

Lin JY (2009). A user's guide to channelrhodopsin variants: features, limitations and future developments. *Exp Physiol* **96**, 19–25.

Machado TA, Pnevmatikakis E, Paninski L, Jessell TM & Miri M (2015). Primacy of flexor locomotor pattern revealed by ancestral reversion of motor neuron identity. *Cell* **162**, 338–350.

Marder E & Calabrese RL (1996). Principles of rhythmic motor pattern generation. *Physiol Rev* **76**, 687–717.

McCrea DA & Rybak IA (2007). Modeling the mammalian locomotor CPG: insights from mistakes and perturbations. *Prog Brain Res* **165**, 235–253.

McCrea DA & Rybak IA (2008). Organization of mammalian locomotor rhythm and pattern generation. *Brain Res Rev* **57**, 134–146.

Molkov YI, Bacak BJ, Talpalar AE & Rybak IA (2015). Mechanisms of left-right coordination in Mammalian locomotor pattern generation circuits: a mathematical modeling view. *PLoS Comput Biol* **11**, e1004270.

Pearson KG & Duysens J (1976). Function of segmental reflexes in the control of stepping in cockroaches and cats. In: *Neural Control of Locomotion*, ed. Herman RM, Grillner S, Stein PSG & Stuart DG, pp. 519–537. Plenum Press, New York.

Rybak IA, Dougherty KJ & Shevtsova NA (2015). Organization of the mammalian locomotor CPG: review of computational model and circuit architectures based on genetically identified spinal interneurons. *eNeuro* **2**, e0069-15.2015 1–21.

Rybak IA, Shevtsova NA & Kiehn O (2013). Modelling genetic reorganization in the mouse spinal cord affecting left–right coordination during locomotion. *J Physiol* **591**, 5491–5508.

Rybak IA, Shevtsova NA, Lafreniere-Roula M & McCrea DA (2006*a*). Modelling spinal circuitry involved in locomotor pattern generation: insights from deletions during fictive locomotion. *J Physiol* **577**, 617–639.

Rybak IA, Stecina K, Shevtsova NA & McCrea DA (2006*b*). Modelling spinal circuitry involved in locomotor pattern generation: insights from the effects of afferent stimulation. *J Physiol* **577**, 641–658.

Sapir T, Geiman EJ, Wang Z, Velasquez T, Mitsui S, Yoshihara Y, Frank E, Alvarez FJ & Goulding M (2004). Pax6 and engrailed 1 regulate two distinct aspects of renshaw cell development. *J Neurosci* **24**, 1255–1264.

Shevtsova NA, Talpalar AE, Markin SN, Harris-Warrick RM, Kiehn O & Rybak IA (2015). Organization of left-right coordination of neuronal ctivity in the mammalian spinal cord: insights from computational modelling. *J Physiol* **593**, 2403–2426.

Stuart DG & Hultborn H (2008). Thomas Graham Brown (1882–1965), Anders Lundberg (1920–), and the neural control of stepping. *Brain Res Rev* **59**, 74–95.

Talpalar AE, Bouvier J, Borgius L, Fortin G, Pierani A & Kiehn O (2013). Dual-mode operation of neuronal networks involved in left-right alternation. *Nature* **500**, 85–88.

Tazerart S, Viemari J-C, Darbon P, Vinay L & Brocard F (2007). Contribution of persistent sodium current to locomotor pattern generation in neonatal rats. *J Neurophysiol* **98**, 613–628.

Tazerart S, Vinay L & Brocard F (2008). The persistent sodium current generates pacemaker activities in the central pattern generator for locomotion and regulates the locomotor rhythm. *J Neurosci* **28**, 8577–8589.

Zhang J, Lanuza GM, Britz O, Wang Z, Siembab VC, Zhang Y, Velasquez T, Alvarez FJ, Frank E & Goulding M (2014). V1 and V2b interneurons secure the alternating flexor-extensor motor activity mice require for limbed locomotion. *Neuron* **82**, 138–150.

Zhong G, Masino MA & Harris-Warrick RM (2007). Persistent sodium currents participate in fictive locomotion generation in neonatal mouse spinal cord. *J Neurosci* **27**, 4507–4518.

Zhong G, Shevtsova NA, Rybak IA & Harris-Warrick RM (2012). Neuronal activity in the isolated mouse spinal cord during spontaneous deletions in fictive locomotion: insights into locomotor central pattern generator organization. *J Physiol* **590**, 4735–4759.

Ziskind-Conhaim L, Wu L & Wiesner EP (2008). Persistent sodium current contributes to induced voltage oscillations in locomotor related Hb9 interneurons in the mouse spinal cord. *J Neurophysiol* **100**, 2254–2264.

Additional information

Competing interests

None.

Author contributions

N.A.S. and I.A.R. designed research; N.A.S. performed simulations; N.A.S. and I.A.R. wrote the paper. Both authors have approved the final version of the manuscript and agree to be accountable for all aspects of the work. All persons designated as authors qualify for authorship, and all those who qualify for authorship are listed.

Funding

This study was supported by National Institutes of Health (NIH) grants NS081713, NS090919, and NS095366.

Acknowledgements

Authors thank Dr Kimberly Dougherty for useful comments and discussion.